Results of Laminar Flow Analysis and Turbulent Flow Experiments for Eccentric Annular Ducts

V. K. JONSSON and E. M. SPARROW

University of Minnesota, Minneapolis, Minnesota

In a paper that recently appeared in the *Journal* (*1*), an analysis of fully developed laminar flow in eccentric annuli was reported.* This same problem was independently and contemporaneously studied by the present authors (*5*), and numerical results were evaluated for a wider range of the governing parameters than in the aforementioned paper. The purpose of this note is to present an expanded set of results for the laminar case and, in addition, to make comparisons with experimental measurements for turbulent flow in eccentric annular ducts (*5*).

The present analysis for laminar flow in eccentric annuli is sufficiently similar to that of reference *1*, so that the details may be omitted here. Attention is immediately directed to the results.

The circumferential distribution of the local wall shear stress τ is shown in Figure 1. The figure consists of four graphs corresponding, respectively, to radius ratios $r_1/r_2 = 0.9$, 0.75, 0.5, and 0.25. In turn, each graph has two parts. The upper part gives shear results for the inner bounding wall (subscript 1) and the lower part gives corresponding results for the outer bounding wall (subscript 2).

The circumferential distributions of τ_1 and τ_2 are plotted as functions of the angles θ_1 and θ_2 that are defined in the inset of the graph. The quantity $\bar{\tau}$ is the overall average wall shear stress, the numerical values of which are found from the friction factors that are presented subsequently. The radius parameters appearing on the ordinates are suggested by the overall force balance

$$\frac{r_1}{r_1 + r_2}\frac{\bar{\tau}_1}{\tau} + \frac{r_2}{r_1 + r_2}\frac{\bar{\tau}_2}{\tau} = 1 \quad (1)$$

in which $\bar{\tau}_1$ and $\bar{\tau}_2$ are the respective averages of $\tau_1(\theta_1)$ and $\tau_2(\theta_2)$. The data points are for turbulent flow and will be discussed later. The eccentricity ϕ is $e/(r_2 - r_1)$. Among the eccentricities investigated, 0.01 and 0.99 were employed in lieu of 0 and 1.0 because the transformation from cartesian to bipolar coordinates is singular at the latter points.

* Other analytical contributions are cited in references 2, 3, and 4.

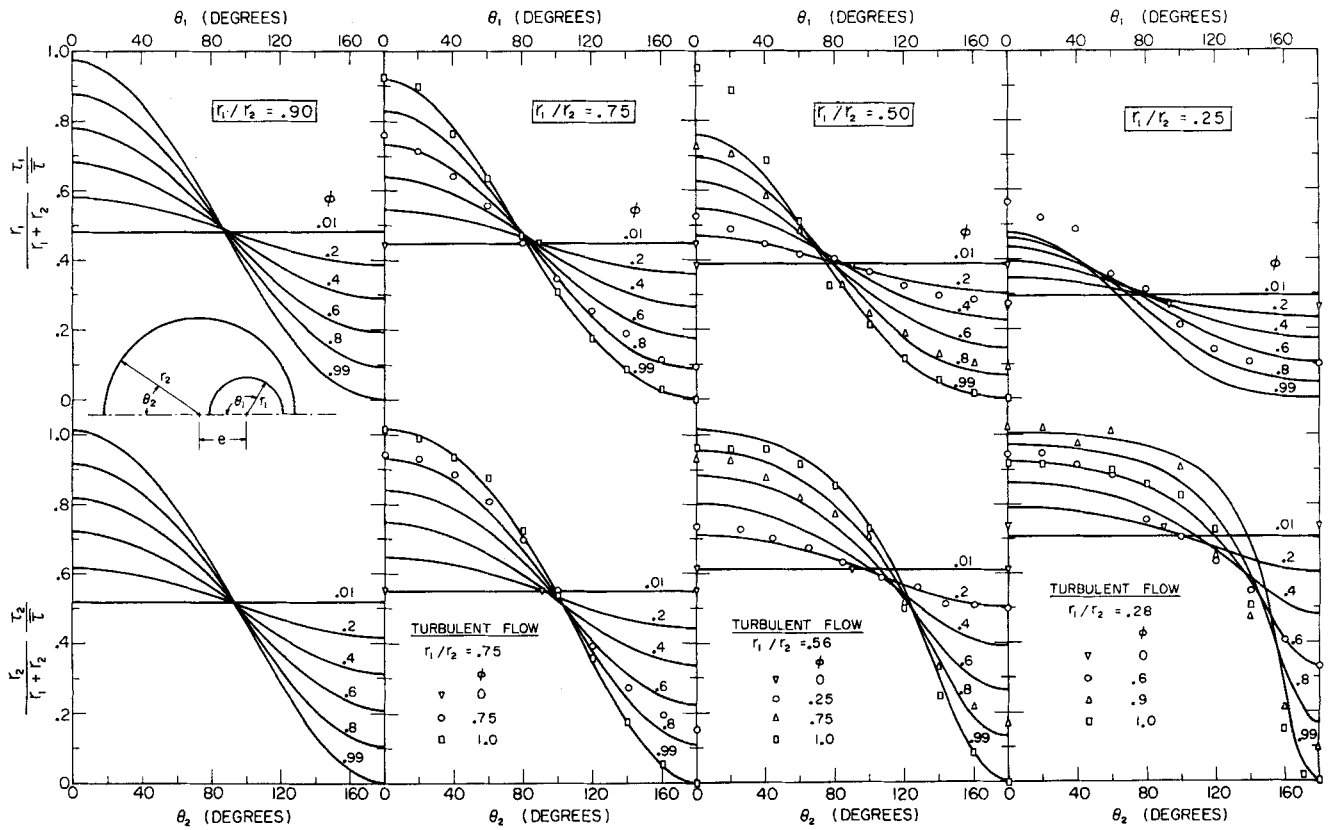

Fig. 1. Circumferential distribution of the local wall shear stress.

INFORMATION RETRIEVAL*

Experimental studies of three-dimensional filtration on a circular leaf, Leonard, J. I., and Howard Brenner, **A.I.Ch.E. Journal, 11,** No. 6, p. 965 (November, 1965).

Key Words: Filtration-8, Three-Dimensional-0, Leaves-10, Circular-0, Shape-8, 7, 9, Filter Cake-9, Compressibility-6, Resistance-6, Filter Cloth-9, Formation-8, Prediction-8, Darcy's Law-10, Pressure Drop-6.

Abstract: The actual shape of a spheroidal filter cake formed on a laterally unconfined circular test leaf was compared with that predicted from theory. In these experiments incompressible cake and filter media of negligible resistance were used. There was a discrepancy between actual and predicted shape. It is speculated that the observed departure from theory may be due to the inapplicability of Darcy's law, especially in the early stages of cake formation.

On finite amplitude roll cell disturbances in a fluid layer subjected to heat and mass transfer, Sani, R. L., **A.I.Ch.E. Journal, 11,** No. 6, p. 971 (November, 1965).

Keywords: Fluid Mechanics-8, Heat Transfer-8, Mass Transfer-8, Determination-8, Stability-8, 9, Nonlinear-0, Hydrodynamic-0, Layer-9, Fluid-9, Perturbation Method-10.

Abstract: The nonlinear aspects of the hydrodynamic stability of a horizontal fluid layer subjected to heat and mass transfer are investigated theoretically. Consideration is restricted to finite amplitude roll cell disturbances. A perturbation method is used to determine the stability of the system as well as the average vertical transport of heat and mass.

Sedimentation of dilute suspensions in creeping motion, Famularo, Jack, and John Happel, **A.I.Ch.E. Journal, 11,** No. 6, p. 981 (November, 1965).

Key Words: Sedimentation-8, 7, 9, Suspensions-9, Agglomeration-6, Creeping Motion Equations-10, Stokes' Settling Velocity-8, Computer-10, Calculation-8, Superposition-10.

Abstract: A superposition technique is employed to obtain a first-order correction to Stokes' settling velocity for dilute suspensions. It is shown that agglomeration can markedly increase settling velocity in the dilute range and hence must be included in theoretical or experimental settling rate equations.

Flow behavior of viscoelastic fluids in the inlet region of a channel, Metzner, A. B., and J. L. White, **A.I.Ch.E. Journal, 11,** No. 6, p. 989 (November, 1965).

Keywords: Analysis-8, Flow-8, 9, 7, Fluids-9, Viscoelastic-0, Dilatant-0, Plates-9, Parallel-0, Flat-0, Rivlin-Ericksen Approximation-10, Viscoelasticity-6, Non-Newtonian-0, Slurries-9.

Abstract: The behavior of viscoelastic fluids in the inlet region of a channel formed by two parallel flat plates has been analyzed with a Rivlin-Ericksen approximation to describe the fluid properties. It is found that viscoelasticity changes the entry length; both the magnitude and direction of this change are predicted to depend upon the detailed fluid properties. These predictions of the change in the entry length are qualitatively supported by available experimental evidence.

* For details on the use of these Key Words and the A.I.Ch.E. Information Retrieval Program, see **Chem. Eng. Progr.,** Vol. 60, No. 8, p. 88 (August, 1964). A free copy of this article may be obtained by sending a post card, with the words "Key Word Article" and your name and address (please print) to Publications Department, A.I.Ch.E., 345 East 47 St., N. Y. N. Y., 10017. Price quotations for volume quantities on request. Free tear sheets of the information retrieval entries in this issue may be obtained by writing to the New York office.

(Continued on page 1146)

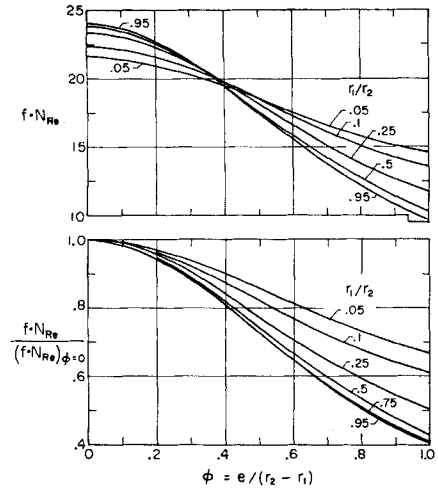

Fig. 2. Friction factor results.

Inspection of the figure reveals that on both walls the largest shear is at the largest gap ($\theta = 0$ deg.) and the smallest shear is at the smallest gap ($\theta = 180$ deg.). For the fully eccentric annulus ($\phi = 1$), the shear is zero at the point of contact of the walls. At the smallest radius ratio, there is a considerable segment of the outer wall on which the shear is uniform.

Results for the overall friction factor f are presented in Figure 2 as the product $f \cdot N_{Re}$, wherein

$$f = \frac{2\bar{\tau}}{\rho \bar{u}^2} = \frac{(-dp/dz)(r_2 - r_1)}{\rho \bar{u}^2},$$

$$N_{Re} = \frac{\rho \bar{u}\, 2(r_2 - r_1)}{\mu} \quad (2)$$

The lower part of the figure shows the friction factor normalized by the corresponding value for the concentric annulus. When plotted in this way, the effects of radius ratio are, in essence, suppressed for $0.5 \leq r_1/r_2 \leq 1.0$. The effect of eccentricity is to decrease the friction factor.

The upper part of the figure shows un-normalized friction factors. It is observed that at small eccentricities $f \cdot N_{Re}$ increases with increasing r_1/r_2. An opposite trend exists at large eccentricities.

It is believed that the values of $f \cdot N_{Re}$ computed in reference *1* ($r_1/r_2 = 5/6$ and $1/2$) are slightly in error at the higher eccentricities. It is found that slow series convergence and small integration step-size are characteristic at large eccentricities. The present results are believed accurate to 0.1 %. For $r_1/r_2 = 5/6$ and $\phi = 0.8$, the $f \cdot N_{Re}$ value from reference *1* exceeds that computed here by 4%.

The experiments that provided the data points of Figure 1 will now be

briefly described (details are available in reference 5). Air was the working fluid. The test section consisted of a 4-in. diameter outer tube and a series of three interchangeable inner tubes. The resulting duct radius ratios were $r_1/r_2 = 0.28$, 0.56, and 0.75. Any value of the eccentricity ϕ could be attained by adjusting the position of the inner tube. The test section was oriented vertically to eliminate the possibility of sag.

The velocity profiles were sensed by a total pressure probe mounted on a traversing mechanism which permitted carefully controlled travel normal to either tube at various angular positions. After the velocity distribution had been measured, constant velocity lines were drawn on a layout of the duct cross section. Then, zero shear lines (that is, gradient lines) were constructed perpendicular to the constant velocity lines. Once such a contour diagram had been completed, the local wall shear stress was found by making a force balance on a control surface composed of gradient lines and the wall. By this technique, the wall shear stress distribution was obtained for the aforementioned radius ratios and for several eccentricities. It was found that the normalized wall shear stress distribution was essentially independent of Reynolds number in the range from 30,000 to 180,000.

The experimental data just described are plotted in Figure 1. At the higher radius ratios, the agreement between the laminar theory and the turbulent data is remarkably good, for the lowest radius ratio, $r_1/r_2 = 0.25$, the agreement is not quite as good. However, the data themselves may contain uncertainties owing to the possible existence of a secondary flow in the cross section. The departure between the laminar and turbulent results at smaller values of r_1/r_2 is consistent with the findings of Brighton and Jones (*6*) for the concentric annulus.

NOTATION

e = distance between centers
f = friction factor
N_{Re} = Reynolds number
p = static pressure
$\bar{u}$ = average velocity
z = axial coordinate

Greek Letters

θ = angular coordinate
μ = dynamic viscosity
ρ = density
τ = local wall shear
$\bar{\tau}$ = average wall shear
ϕ = eccentricity

Subscripts

1 = inner wall
2 = outer wall

LITERATURE CITED

1. Snyder, W. T., and G. A. Goldstein, *A.I.Ch.E. J.*, **11**, 462 (1965).
2. Caldwell, A., *J. Roy. Tech. Coll. Glasgow*, **2** (1930).
3. Piercy, N. A. V., M. S. Hooper, and H. F. Winny, *Phil. Mag. Ser. 7*, **15**, 617 (1933).
4. Dryden, H. L., F. D. Murnaghan, and Harry Bateman, "Hydrodynamics," p. 198, Dover, New York (1956).
5. Jonsson, V. K., Ph.D. thesis, Univ. Minnesota, Minneapolis (1965).
6. Brighton, J. A., and J. B. Jones, *J. Basic Eng.*, **D86**, 835 (1964).

Nonequilibrium, Inverse Temperature Profile in Boiling Liquid-Metal Two-Phase Flow

JOHN C. CHEN

Brookhaven National Laboratory, Upton, New York

The results of recent experiments with boiling two-phase flow of potassium indicate the existence of an inverse temperature profile in the two-phase fluid. This note presents some of the results and a theoretical explanation for this phenomenon.

EXPERIMENT

Wall and fluid temperatures were measured for vertical axial flow of potassium vapor and liquid through a boiling section. As shown in Figure 1, twelve thermocouples were used to measure temperatures at various radial positions in the boiler wall, and three immersion thermocouples located at the axis of the pipe were used to measure the fluid temperature. The test section was installed in a pumped loop which supplied potassium vapor-liquid mixtures at controlled temperatures, pressure, flow rates, and qualities.

Figure 2 shows temperature data collected for three sample boiling runs. Temperatures measured in the wall and in the fluid are plotted against the log of the radial position. Runs B-12b and B-9b represent the "normal" situation where the I.D. wall temperature is higher than the fluid temperature. Run B-11b represents the unexpected situation where the wall temperature is lower than the fluid center line temperature. This inverse temperature profile actually was found for a majority of the runs in this particular series of tests. The range of variables covered in the test were: flow rate—0.9 to 4.9 gpm, potassium temperature—1,510° to 1,650°F., boiling pressure—28 to 42 lb./sq. in. abs., vapor quality—0.7 to 17.0%, and boiling heat flux—10,200 to 81,700 B.t.u./(hr) (sq. ft.) The measured difference between I.D. wall temperature and fluid core temperature ($T_w - T_o$) ranged from +4.2° to −9°F.

The runs with negative temperature differences were first thought to be in error, but repeated checks of the experi-